



## Facile synthesis of tetrapodal ZnO nanoparticles by modified French process and its photoluminescence

Tawatchai Charinpanitkul<sup>a,b,\*</sup>, Pat Nartpochananon<sup>a</sup>, Thornchaya Satitpitakun<sup>a</sup>, Jenifer Wilcox<sup>c</sup>, Takafumi Seto<sup>d</sup>, Yoshio Otani<sup>d</sup>

<sup>a</sup> Center of Excellence in Particle Technology, Faculty of Engineering, Chulalongkorn University, Bangkok, Thailand

<sup>b</sup> Energy Research Institute, Chulalongkorn University, Bangkok, Thailand

<sup>c</sup> Department of Energy Resources Engineering, Stanford University, CA, USA

<sup>d</sup> Department of Chemical Engineering, Faculty of Engineering, Kanazawa University, Kanazawa, Japan

### ARTICLE INFO

#### Article history:

Received 2 March 2011

Accepted 27 May 2011

Available online 7 November 2011

#### Keywords:

ZnO

Nanoparticles

Photoluminescence

Nucleation

Oxidation

### ABSTRACT

Facile synthesis of tetrapodal ZnO nanoparticles was conducted using a modified French process in which oxygen and nitrogen flow rates were controlled. The synthesized ZnO nanoparticles exhibit photoluminescent characteristics depending on the synthesis conditions. Electron microscopic analysis revealed that the tetrapodal nanostructure of ZnO with high crystallinity which was confirmed by XRD analyses could be controlled by a variation of O<sub>2</sub>/N<sub>2</sub> feed ratio. Typical photoluminescence with UV and blue emission of the tetrapodal ZnO nanoparticles was influenced by the particle size and crystallinity, which is manipulated by the oxidation condition.

© 2011 The Korean Society of Industrial and Engineering Chemistry. Published by Elsevier B.V. All rights reserved.

### 1. Introduction

Among various advanced materials, zinc oxide (ZnO) is recognized as an n-type semiconductor with a wide band gap of 3.37 eV and large exciton binding energy of 60 meV [1–8], leading to extensive studies in many promising applications, such as room-temperature UV laser [2], field emission [3], photoluminescence [4], photocatalyst [5], superhydrophilic coating [6] and dye-sensitized solar cell [7]. Based on those previous works, for instance, transparency of hydrophilic ZnO thin film would be controlled by the size of ZnO. Also, improvement of ZnO size distribution would significantly improve efficiency of DSSC with photoelectrodes containing of ZnO nanoparticles. Thereby, there are increasing attempts to develop various alternative techniques for the mass production of ZnO nanoparticles with controllable characteristics [3–9]. So far, most of previous investigations on the synthesis of ZnO nanoparticles have been conducted via wet chemistry route. However, it is well recognized that the industrial-scale production of ZnO particles is generally conducted using a

French process in which high purity zinc ingot is vaporized before being oxidized by an excessive air supply. The synthesized ZnO particles could be entrained by the air flow of which the O<sub>2</sub> concentration is gradually decreased while it flows through the conveying duct. The natural quenching would also result in the polydispersity of the synthesized ZnO nanoparticles which would uncontrollably grow to larger agglomerates with typical size of many micrometers. Such a fact suggests that it is difficult to control the characteristics of ZnO particles synthesized by the normal French process. Therefore, requirement of other alternatives which could provide a control of oxidation of zinc vapor and agglomeration of ZnO nucleates would be an important issue worthwhile for further investigation. It is reasonable that the oxidation of zinc vapor would be regulated by the controlled supply of O<sub>2</sub> into the synthesizing system. Therefore, a French process with a modification of O<sub>2</sub> and N<sub>2</sub> gas supply is proposed and examined.

It could be emphasized that the prime importance of this work is the usage of the modified French process in which O<sub>2</sub> and N<sub>2</sub> gas supply is precisely controlled, resulting in a uniform generation of tetrapodal ZnO nanoparticles with high crystallinity and relatively narrow size distribution. The morphological and photoluminescent characteristics of the synthesized tetrapod ZnO nanoparticles which could be verified by microscopic and spectroscopic analyses were discussed with a proposed mechanism of their formation.

\* Corresponding author at: Center of Excellence in Particle Technology, Faculty of Engineering, Chulalongkorn University, Bangkok, Thailand. Tel.: +66 2 2186480; fax: +66 2 2186480.

E-mail address: [ctawat@chula.ac.th](mailto:ctawat@chula.ac.th) (T. Charinpanitkul).

## 2. Experimental

In this work, the facile synthesis of ZnO nanoparticles with a modified French process was conducted using a custom-fabricated reactor which is schematically shown in Fig. 1. The quartz tube reactor with a volume of  $19.8 \times 10^{-4} \text{ m}^3$  (I.D. of  $6.0 \times 10^{-2} \text{ m}$  and length of  $0.7 \text{ m}$ ) is partitioned into 3 zones consisting of (1) zinc-vaporizing zone ( $12 \times 10^{-2} \text{ m}$ ) equipped with an electrical heater, (2) reaction zone ( $8 \times 10^{-2} \text{ m}$ ) and (3) well-insulated product-removing zone ( $50 \times 10^{-2} \text{ m}$ ). With a steady heating rate of  $50 \text{ }^\circ\text{C}/\text{min}$  the reactor temperature was increased from the ambient temperature to  $900 \text{ }^\circ\text{C}$  and kept constant for 30 min to confirm that 2 g of pure zinc powder (99% purity, Merck) is totally vaporized under the atmospheric pressure similar to that in the conventional French process.  $\text{N}_2$  gas with a regulated flow rate of 1000 or 2000 mL/min is fed to carry zinc vapor into the reaction chamber in which a cool  $\text{O}_2$  stream with a designated flow rate (10 and 20 mL/min) is supplied. A key issue of this work is the control of the partial pressure of  $\text{O}_2$  by varying the  $\text{N}_2/\text{O}_2$  feed ratio, which is essential for the oxidation of zinc vapor. Particulate matter generated as a product species could be withdrawn and collected using a flash trap connected with a vacuum pump.

Repetitive samples of the synthesized tetrapod ZnO nanoparticles were characterized using a field emission scanning electron microscopy (FESEM, Hitachi S-900), X-ray diffractometry with  $\text{Cu K}\alpha$  radiation (XRD, Bruker AXS-D8), particle size analyzer (Malvern Mastersizer2000) and a room temperature photoluminescence spectrometry (JASCO FP-6200) using a Xe lamp with an excitation wavelength of 325 nm.

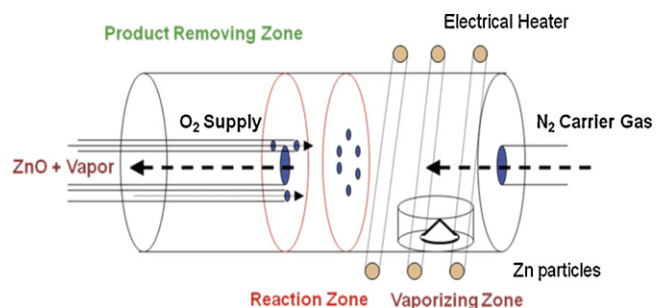


Fig. 1. Schematic diagram of originally designed tubular reactor.

## 3. Results and discussion

Typical SEM images of particulate products synthesized with a varied  $\text{N}_2/\text{O}_2$  feed ratio are illustrated in Fig. 2. In referring experiments without  $\text{O}_2$  feed, a room-temperature  $\text{N}_2$  stream with a flow rate of 10 mL/min was fed into the reaction zone, resulting in the formation of gray particulate products. Regarding to SEM analysis shown in Fig. 2(a), irregular structure of zinc nanoparticles was synthesized. Such morphology would be attributed to fast crystallization of saturated zinc vapor after contacting with the colder stream of  $\text{N}_2$  [8]. On the other hand, when a 10 mL/min  $\text{O}_2$  flow was supplied with a  $\text{N}_2$  flow of 1000 mL/min, gray-white particulate product was obtained. Typical micrograph in Fig. 2(b) reveals that the synthesized product mainly consisted of tetrapodal nanoparticles with a uniform size. Additionally as shown in Fig. 2(c), the further increase in  $\text{O}_2$  flow to 20 mL/min with a

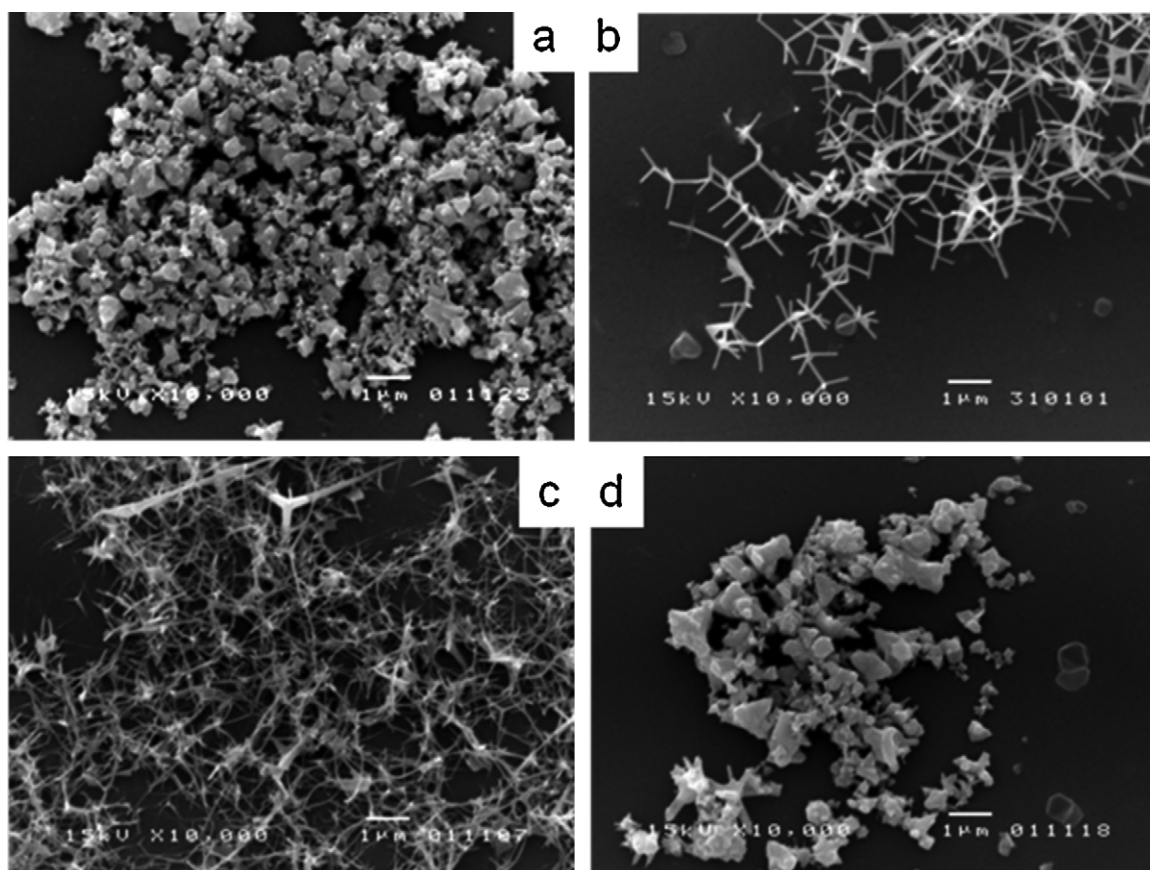


Fig. 2. Typical SEM images of as-synthesized particulate products obtained with different  $\text{O}_2/\text{N}_2$  flow ratio: (a) 0/1000, (b) 10/1000, (c) 20/1000 and (d) 20/2000 mL/min.

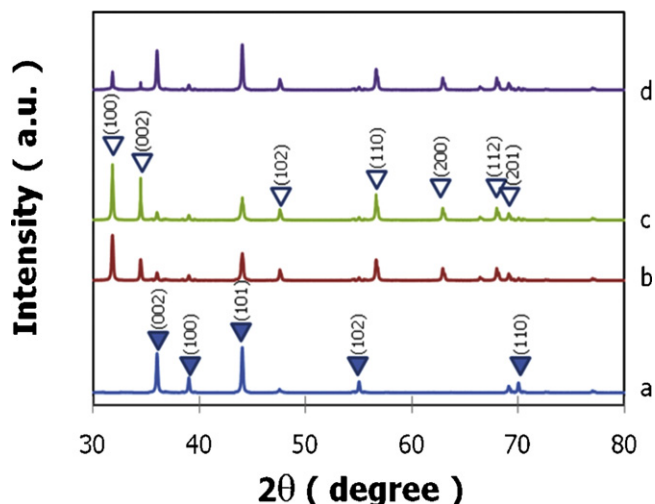


Fig. 3. XRD pattern of each as-synthesized particulate product depicted in Fig. 2.

constant  $N_2$  flow could provide tetrapodal nanoparticles with much longer and thicker pods, resulting in a broader size distribution. However, a further increase in the  $N_2$  flow to 2000 mL/min with the 20 mL/min  $O_2$  flow resulted in a gray-white product which was a mixture of coarse tetrahedral nanoparticles and a small amount of thick tetrapodal nanoparticles as shown in Fig. 2(d).

All particulate samples were also characterized by recording its XRD patterns as shown in Fig. 3(a)–(d). Based on curve (a), strong peaks at  $2\theta = 36.05^\circ$ ,  $39.64^\circ$ ,  $44.32^\circ$ ,  $55.85^\circ$  and  $70.45^\circ$  assigned respectively to (0 0 2), (1 0 0), (1 0 1), (1 0 2) and (1 1 0) planes confirms that the particulate products were mainly composed of pure Zn particles with polycrystalline hexagonal characteristics [10]. Meanwhile, XRD patterns (b) and (c) indicate that the purely white products synthesized by the  $O_2$  flow rate increased from 10

to 20 mL/min with the constant  $N_2$  flow of 1000 mL/min consist of ZnO with tetrapodal nanostructures in wurtzite hexagonal phase (wurtzite-type, space group P63mc, JCPDS 36–1451) with representative peaks at  $2\theta = 31.85^\circ$ ,  $34.38^\circ$ ,  $47.45^\circ$ ,  $57.58^\circ$ ,  $66.35^\circ$ ,  $67.91^\circ$  and  $69.02^\circ$  referring to (1 0 0), (0 0 2), (1 0 2), (1 1 0), (2 0 0), (1 1 2) and (2 0 1) planes, respectively. It is noted that weak peaks of (1 0 1), (0 0 2) and (1 0 0) of Zn were also observed in both ZnO samples. Furthermore, the further increase in  $N_2$  flow to 2000 mL/min resulted in a different XRD pattern containing ZnO peaks and enhanced peaks of zinc.

Based on the abovementioned analytical results, the possible formation mechanisms of Zn and ZnO nanoparticles is proposed as depicted in Fig. 4(a)–(c). As depicted in Fig. 4(a), tetrahedral Zn nanoparticles would be synthesized due to the supersaturation of Zn nucleates which undergo the self-assembling process without the  $O_2$  supply when they come to the low temperature zone by the nitrogen flow [2,3]. When the  $O_2$  with a lower temperature is supplied into the reactor, nucleates of ZnO could be produced because of the oxidation of zinc vapor which is carried over by the oxygen and nitrogen flow. Wurtzite hexagonal pod of ZnO would grow from the tetrahedral faces of their nucleates, resulting in the tetrapodal structure of ZnO nanoparticles as depicted in Fig. 4(b) [5,11]. On the other hand, ZnO nanoparticles could be generated while some zinc nanoparticles are also produced when a higher  $N_2$  flow is supplied to dilute the oxygen concentration, which is attributed to the incomplete oxidation [11]. In addition, the higher total gas flow rate would proportionally reduce the residence time of zinc vapor within the reaction zone, leading to a mixed formation of Zn and ZnO nanoparticles as illustrated in Fig. 4(c). The higher gas flow rate would enhance the turbulent mixing, resulting in the higher collision of the growing seeds of Zn and ZnO via the competitive process which is controlled by the partial pressure of  $O_2$  in the reaction zone [11,12]. Therefore, with the excessive  $N_2$  supply the formation of Zn nanoparticles of which melting temperature is lower would become dominant, leading to the agglomeration of synthesized nanoparticles. Therefore, it

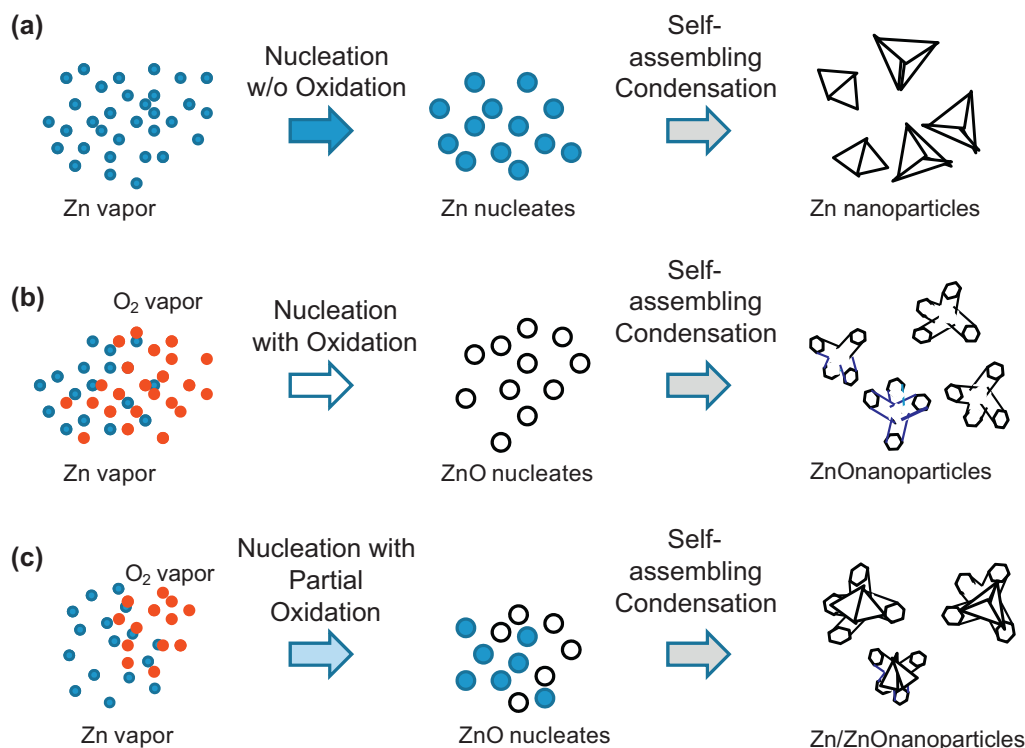
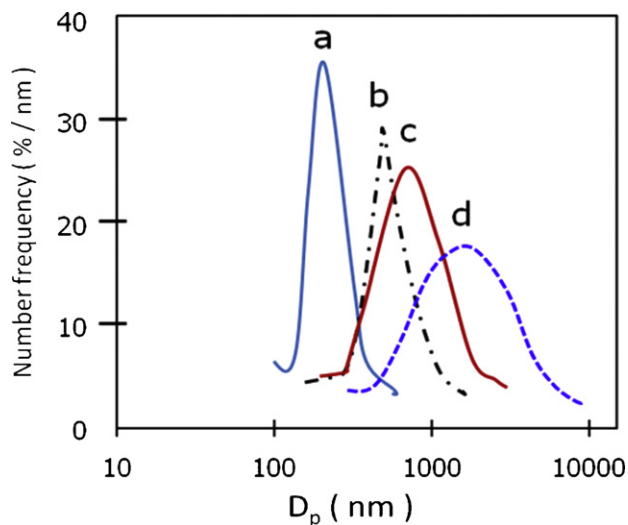


Fig. 4. Possible mechanism of Zn and ZnO nanoparticle formation under different oxidizing condition. (a) Without oxidation, (b) with oxidation and (c) with partial oxidation.



**Fig. 5.** Particle size distribution (PSD) of each as-synthesized particulate product depicted in Fig. 2.

should be noted that within the specially designed reactor, the self assembling method could be controlled by the regulation of  $O_2$  and  $N_2$  flows, leading to Zn and ZnO nanoparticles with distinctively different morphologies.

All repetitive samples were further characterized for their particle size distribution by the particle size analyzer as depicted in Fig. 5. Each distribution corresponds to the as-synthesized nanoparticles which were analyzed by SEM microscopy. Sample (a) which mainly contains tetrahedral particles exhibits the narrowest distribution with a modal size of 210 nm. Tetrapodal ZnO nanoparticles synthesized by supplying  $O_2$  flow rates of 10 and 20 mL/min exhibit broader particle size distribution with an average particle size of 520 and 610 nm, respectively. Regarding sample (d) which was synthesized with the highest total gas flow rate, the ZnO nanoparticles with the broadest particle size distribution an average particle size of 1800 nm were obtained. These results would also confirm the formation of agglomerates of Zn and ZnO would be more enhanced with the excessive total gas flow as described by the XRD analyses.

In term of production rate, it was found that an oxygen/nitrogen supply with a volume ratio of 10/1000 could provide particulate product with gray color in an average amount of 1.2 g. With regarding to microscopic and spectroscopic analyses shown in Figs. 1 and 2, it would be able to imply that the amount of synthesized ZnO would be lower than 0.9 g. With the increased oxygen/nitrogen flow rate ratio to 20/1000, it could be clearly observed that purely white particulate product with an average weight of 1.5 g could be synthesized. However, with the oxygen/nitrogen flow rate ratio of 20/2000 the amount of synthesized product drastically decreased to 0.6 g. This would be attributed to the higher entrainment of synthesized product due to the excessively high carrier gas flow rate [8]. It should be noted that analysis of ZnO purity in the synthesized product would be further conducted for improving the synthesizing yield.

Furthermore, photoluminescent (PL) spectra of ZnO nanoparticles synthesized at different oxidation conditions are analyzed and illustrated in Fig. 6. It was found that Zn nanoparticles prepared under the condition without  $O_2$  supply did not exhibit detectable PL characteristics [10]. For all product samples synthesized with the  $O_2$  supply, two unique emission bands which are an ultraviolet emission band at 383–399 nm and a blue emission band at 440–490 nm could be detected. In general, low temperature UV photoluminescence (PL) of ZnO

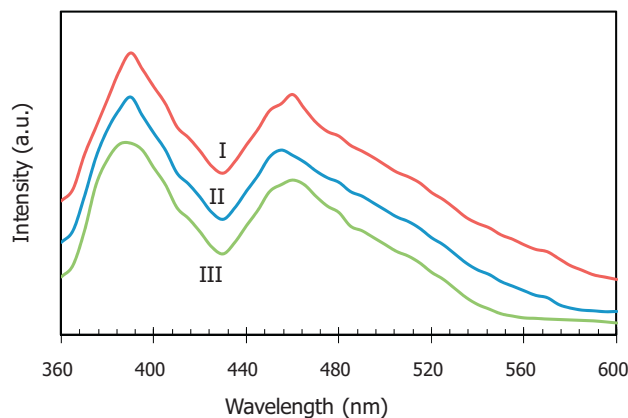


**Fig. 6.** Photoluminescence spectrum of ZnO particles synthesized with different  $O_2/N_2$  flow ratio: I = 10/1000, II = 20/1000 and III = 20/2000.

could be more enhanced by the recombination of free excitons when it is in nanostructures [12]. Therefore, the UV emission of our synthesized samples would be a good evidence of the existence of rather high quality ZnO nanoparticles. With the low  $O_2$  supply, spectrum I shows the sharp UV emission band, possible due to their smaller size [9,13]. In spectrum II, the UV intensity increases with the increased  $O_2$  flow rate because more ZnO nanoparticles could be generated from enhanced oxidation of Zn vapor. However, with an increase in the  $N_2$  flow rate, the UV emission peaks in spectrum III exhibit a red-shift which would be ascribed to larger particle size [14]. Meanwhile, there exists another blue emission band with the center at 459 nm or equivalent to 2.7 eV, attributed to the presence of some defects which would be resulted from oxygen vacancies and interstitial zinc [15]. According to Zeng et al., the defect energy level of interstitial zinc is about 0.22 eV below the conduction band edge while the band gap of ZnO is 3.31 eV [16]. Those reported results are in a good agreement with the energy of the blue PL observed in this work; therefore, the blue PL emission of the synthesized ZnO nanoparticles would be attributed to interstitial zinc at the surface which could also be confirmed using SEM.

In summary, the modified French process using a custom-built reactor, which is applicable for the control of  $O_2/N_2$  feed ratio leading to the controlled synthesis of ZnO nanoparticles with uniform size, crystallinity and photoluminescence characteristics. Also, the increase in  $O_2$  supply could enhance the dominating growth of tetrapodal ZnO nanoparticles, while the increased flow of the entrained- $N_2$  stream would provide the incomplete oxidation of zinc vapor, resulting in the formation of interstitial zinc on the surface of the synthesized ZnO nanoparticles then enhanced the blue PL emitting characteristics.

#### 4. Conclusion

In this work ZnO nanoparticles could be synthesized by the modified French method within the uniquely fabricated reactor which could provide manipulation of  $O_2$  and  $N_2$  gas flow rate. ZnO nanoparticles synthesized with the lower  $O_2/N_2$  feed ratio exhibited the uniform tetrapodal nanostructure with high crystallinity. The increase in the  $O_2$  supply would lead to further growth of tetrapodal ZnO nanoparticles, consequently resulting in the stronger UV and blue PL emission. However, the excessive  $N_2$  flow would lead to the shorter residence time of reactive zinc vapor and the agglomeration of coarse Zn and ZnO nanoparticles. Thereby the particulate products synthesized with the excessive  $N_2$  flow would exhibit the interstitial surface-bound zinc, which preferably enhance the blue PL emitting characteristics.

## Acknowledgements

Supports from the Centenary Fund of Chulalongkorn University and NANOTEC to CEPT are gratefully acknowledged. KUSEP scholarships for P.N. and T.S. are also acknowledged.

## References

- [1] E.M. Wong, P.C. Searson, *Appl. Phys. Lett.* 74 (1999) 2939.
- [2] M.H. Huang, S. Mao, H. Feick, H. Yan, Y. Wu, H. Kind, E. Weber, R. Russo, P. Yang, *Science* 292 (2001) 1897.
- [3] W.Z. Wang, B.Q. Zeng, J. Yang, B. Poudel, J.Y. Huang, M.J. Naughton, Z.F. Ren, *Adv. Mater.* 18 (2006) 3275.
- [4] L. Juhyun, C. Jinho, N. Keeppung, K. Misook, *J. Ind. Eng. Chem.* 15 (2009) 645.
- [5] E.S. Jang, J.H. Won, S.J. Hwang, J.H. Choy, *Adv. Mater.* 18 (2006) 3309.
- [6] P. Numpud, T. Charinpanitkul, W. Tanthapanichakoon, *J. Ceram. Soc. Jpn.* 116 (2008) 414.
- [7] L. Dupuy, S. Haller, J. Rousset, F. Donsanti, J.-F. Guillemoles, D. Lincot, F. Decker, *Electrochem. Commun.* 12 (2010) 697.
- [8] J. Klanwan, N. Akrapattangkul, V. Pavarajarn, T. Seto, Y. Otani, T. Charinpanitkul, *Mater. Lett.* 64 (2010) 80.
- [9] Q. Ahsanulhaq, J.H. Kim, N.K. Reddy, Y.B. Hahn, *J. Ind. Eng. Chem.* 14 (2008) 578.
- [10] G. Kenanakis, E. Stratakis, K. Vlachou, D. Vernadou, E. Koudoumas, N. Katsarakis, *Appl. Surf. Sci.* 254 (2008) 5695.
- [11] Y. Zhang, B. Lin, X. Sun, Z. Fu, *Appl. Phys. Lett.* 86 (2005) 131910.
- [12] S. Cho, J. Ma, Y. Kim, Y. Sun, G.K.L. Wong, J.B. Ketterson, *Appl. Phys. Lett.* 75 (1999) 2761.
- [13] M.K. Lee, H.F. Tu, *J. Jpn. Appl. Phys.* 47 (2008) 980.
- [14] S. Ramanathan, S. Patibandla, S. Bandyopadhyay, J.D. Edwards, J. Anderson, *J. Mater. Sci. Mater. Electron.* 17 (2006) 651.
- [15] B.X. Lin, Z.X. Fu, Y.B. Jia, *Appl. Phys. Lett.* 79 (2001) 943.
- [16] H.B. Zeng, W.P. Cai, J.L. Hu, G.T. Duan, P.S. Liu, Y. Li, *Appl. Phys. Lett.* 88 (2006) 171910.